Available online at www.sciencedirect.com
ScienceDirect
Thermochimica Acta 465 (2007) 83–87
thermochimica acta
www.elsevier.com/locate/tca

Thermophysical properties of the Ni-based alloy Nimonic 80A up to 2400 K, III

B. Wilthan [a,*], R. Tanzer [b], W. Schützenhöfer [b], G. Pottlacher [a]

[a] *Institute of Experimental Physics, Graz University of Technology, Petersgasse 16, 8010 Graz, Austria*
[b] *Böhler Edelstahl GmbH, Mariazellerstrasse 25, 8605 Kapfenberg, Austria*

Received 12 April 2007; received in revised form 29 August 2007; accepted 20 September 2007
Available online 1 October 2007

Abstract

Nimonic 80A is a nickel–chromium alloy which is strengthened by additions of titanium and aluminum. The alloy is used for high temperature, high-strength applications. This superalloy is used in gas turbine hot section components, for hot-working applications and forging hammers.

This is the third paper reporting thermophysical properties of Nimonic 80A. The optical measurement of temperature is limited by our fast pyrometers with T_{min} = 1200 K for this material and data above about 1200 K have been reported in the previous papers [1,2].

Specific heat capacity data from 500 K up to 1500 K obtained by direct measurement using a differential scanning calorimeter have been used to compute enthalpy as function of temperature.

By combining pulse heating and DSC measurements now it is possible to assign a temperature to electrical resistivity and thermal conductivity in the observed temperature range. Thermal conductivity is estimated using the Wiedemann–Franz law.

The investigated specific heat capacity, enthalpy, resistivity and thermal conductivity data as function of temperature are presented and compared to literature-values.

Keywords: Thermophysical properties; Nimonic 80A; Resistivity; Enthalpy; Heat capacity; Thermal conductivity; Thermal diffusivity

1. Introduction

Several thermophysical data for the solid and liquid material have been measured and presented for temperatures above 1100 K in previous papers [1,2]

Within this paper new calorimetric measurements are presented and combined with pulse heating data, where no signal was available from the pyrometer used for the optical temperature measurement.

Data in the solid phase of Nimonic 80A are discussed and compared to literature data, if available. Table 1 gives an overview of the properties of the measured alloy —a typical chemical composition, liquidus temperature, and solidus temperature as specified by Böhler Edelstahl GmbH. The density d at room temperature was determined by turning a cylinder with maximum machine accuracy with the dimensions of about 50 mm in diameter and 50 mm height, measuring and weighing it.

2. Experimental method

To perform accurate specific heat capacity (c_p) measurements of our samples a differential scanning calorimeter (DSC) Netzsch DSC 404 was used for obtaining data in the temperature range of about 500–1500 K. The calculated specific enthalpy H is set to zero at room temperature, 298 K. From the first datapoint to room temperature the c_p value is extrapolated from a linear fit of the mean value of the c_p-data of the first and second run in the temperature range of 480–800 K.

For all of the four different samples with a mass between 109.9 and 173.3 mg a heating rate of 20 K min^{-1} and a sapphire standard was used.

All electrical data presented in this work are obtained by the means of a fast pulse heating technique which is described

* Corresponding author.
E-mail address: wilthan@tugraz.at (B. Wilthan).

0040-6031/$ – see front matter © 2007 Elsevier B.V. All rights reserved.
doi:10.1016/j.tca.2007.09.006

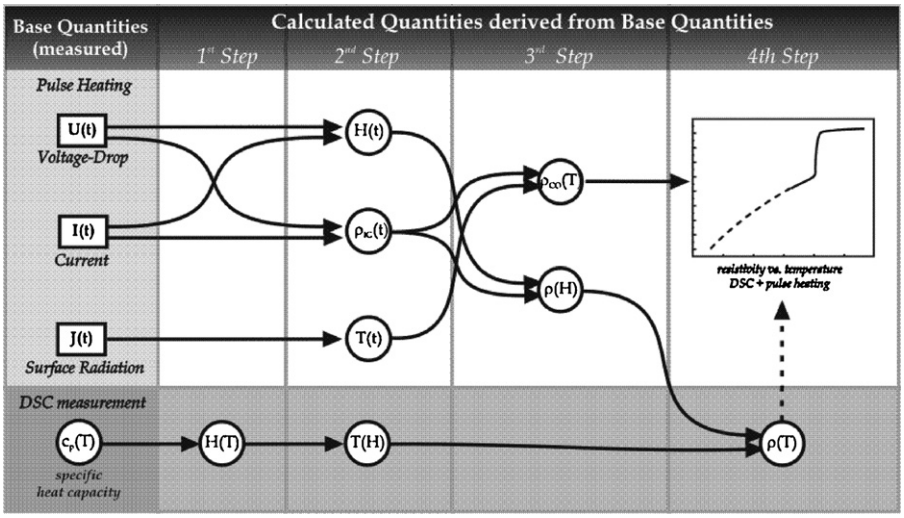

Fig. 1. Schematic overview how pulse heating data are combined to DSC data.

detailed in Refs. [3–5]. Within this setup a time-dependent temperature measurement is performed with a spectral pyrometer developed at the Institute of Experimental Physics (Graz University of Technology) at a wavelength of 1570 nm and a bandwidth (FWHM) of 84 nm. Due to the lack of intensity at low temperatures the working temperature for this pyrometer starts at about 1250 K.

Below this temperature only electrical data namely current, voltage from the pulse heating experiments are used to determine electrical resistivity ρ as function of specific enthalpy.

Incorporating the relation of enthalpy – temperature measured by the DSC – it is possible to assign a temperature to the resistivity data via specific enthalpy. A short overview of the calculated quantities derived from base quantities is given in Fig. 1.

To compensate the volume expansion of the sample in the low temperature range an interpolation of the polynomial fit (Eq. (1)) of density d (kg m^{-3}) versus temperature T(K) between room temperature and the first datapoint at 1100 K is used from the data already published [2].

$$\mathrm{d}(T) = 8251.0 + 1.01 \times 10^{-2} T - 2.845 \times 10^{-4} T^2 \quad 1100\,\mathrm{K} < T < 1593\,\mathrm{K} \tag{1}$$

Thermal conductivity λ is estimated via the Wiedemann–Franz law (Eq. (2)) which states that the ratio of the thermal conductivity to the electrical conductivity $1/\rho$ of a metal is proportional to the temperature:

$$\lambda(T) = \frac{LT}{\rho(T)} \tag{2}$$

where L is the Lorentz number, $L = 2.45 \times 10^{-8}\,\mathrm{V^2\,K^{-2}}$ [3], assuming that the Lorentz number is invariant within the region of interest.

Table 1
Material properties of Nimonic 80A

Name	Nimonic 80A
Composition	Ni, balance; Cr, 19.5%; Ti, 2.5%; Al, 1.7%; Fe, max. 1.5%
T_{solid} (K)	1593
T_{liquid} (K)	1638
Density, 20 °C (kg m^{-3})	8152

3. Results und discussion

Curves obtained for the apparent specific heat capacity (c_p) from the DSC measurement at two identical temperature profiles are illustrated in Fig. 2 in the temperature range 500 K < T < 1500 K. According to the definition of specific heat capacity, where contributions from phase transitions are not included, the given data include all these deviations. All marked

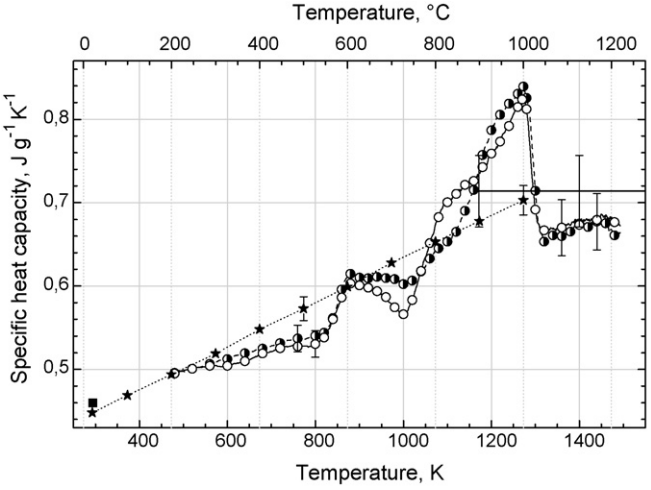

Fig. 2. Specific heat capacity from DSC measurements. (open circles) First run; (half filled circles) second run; (full line) c_p from slope of $H(T)$ by pulse heating; (connected stars) calculated values from Betteridge and Heslop [6]; (full square) single value at room temperature from ASM Handbook [7].

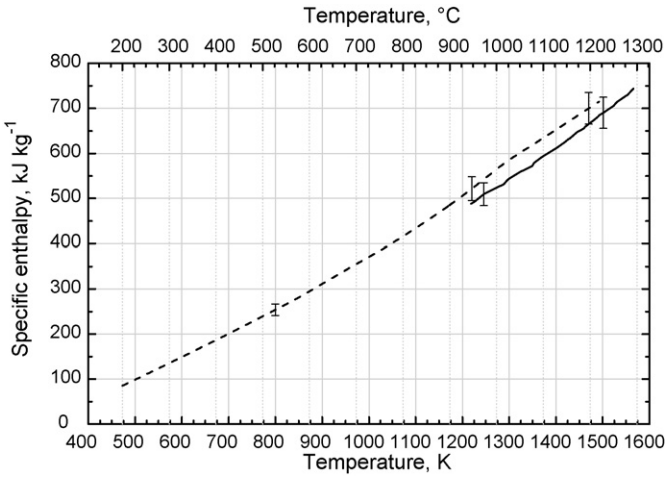

Fig. 3. Specific enthalpy in the solid state. (dashed line) DSC measurement; (full line) pulse heating data.

datapoints in the graph are measured in this study and given in Table 1.

The full line relates to the mean value of all four samples of the first run, the dashed line to the second run in the DSC. Both local maxima at about 880 and 1270 K in the two curves indicate resolution of precipitations of the γ′ phase and carbides. At higher temperatures the γ′ phase is completely dissolved and the specific heat reverts to the normal value, lying approximately on the prolongation of the smooth portion of the curve between 500 and 800 K. The cubic face centered lattice of Nimonic 80A is stable in the solid phase and no phase transitions appear. Differences between the two heating cycles occur due to different states of the materials microstructure. While the first DSC-run describes the material as-received the second run is affected by the heat treatment of the preceded measurement. The constant c_p value plotted as full line is determined from the slope of the specific enthalpy from the pulse heating experiments. One can see that this is a good estimation for a short temperature range before melting. Literature data from Betteridge and Heslop [6] present calculated values of specific heat for Nimonic 80A. The formula used in this work assumes, that there is a linear change in specific heat with temperature and that the effect of precipitated phases is not highly significant. The actual results depict that this assumption is not strictly correct. However, the comparison shows good agreement between the measured and calculated data. A second source [7] reports one value at room temperature and is also listed in Fig. 4 (Table 2).

By integrating the specific heat with respect to temperature T the specific enthalpy H is obtained as function of temperature and depicted in Fig. 3. Data of both methods used, namely DSC and pulse heating measurements, are available between 1250 K, the lowest working temperature for the pyrometer used, and 1500 K, the maximum temperature for the DSC. In this temperature range the results from DSC measurement are about 8% higher than the enthalpy values from the pulse heating experiment.

Phase transitions can easily be observed with DSC measurements, but can be wholly or partially suppressed in the solid phase under pulse-heating conditions as applied within this experiment, due to the extreme high heating rates of 10^8 K s^{-1}. This may also be the reason for the difference in specific enthalpy between data from DSC and pulse heating measurement taking into account the change in material as it can be seen in the c_p-curve.

Table 2
Specific heat capacity from DSC measurement; given data are mean values of four different samples

First run		Second run	
T (K)	c_p (J/g K)	T (K)	c_p (J/g K)
480	0.49500	480	0.49575
520	0.50075	520	0.50075
560	0.50425	560	0.50650
600	0.50425	600	0.51225
640	0.50975	640	0.51950
680	0.51925	680	0.52500
720	0.52550	720	0.53150
760	0.52750	760	0.53700
800	0.53050	800	0.54025
820	0.53825	820	0.54400
840	0.56000	840	0.56150
860	0.58625	860	0.59575
880	0.60300	880	0.61450
900	0.60075	900	0.61000
920	0.59800	920	0.60925
940	0.59375	940	0.61100
960	0.58675	960	0.60950
980	0.57450	980	0.60825
1000	0.56600	1000	0.60225
1020	0.58325	1020	0.60650
1040	0.61800	1040	0.61725
1060	0.65150	1060	0.63300
1080	0.68275	1080	0.64525
1100	0.70050	1100	0.65325
1120	0.71050	1120	0.66500
1140	0.72125	1140	0.69025
1160	0.72600	1160	0.71525
1180	0.74275	1180	0.75725
1200	0.75900	1200	0.78675
1220	0.77325	1220	0.80550
1240	0.79200	1240	0.81875
1260	0.81475	1260	0.83050
1270	0.82390	1273	0.83935
1280	0.81225	1280	0.82550
1300	0.69175	1300	0.71425
1320	0.66675	1320	0.65325
1360	0.67000	1360	0.65975
1400	0.67325	1400	0.67475
1440	0.67950	1440	0.67725
1480	0.67650	1480	0.66075

In Fig. 4, specific electrical resistivity (ρ) is presented for the solid phase. In the temperature range 500 K < T < 1500 K the electrical signals of the pulse heating experiments are used and temperature is assigned via specific enthalpy from the DSC data.

The lower dashed curve represents resistivity without considering volume expansion (index IG) and has an overlap with a full line, where only data from pulse heating are depicted (for fits see Refs. [1,2]).

The dashed dotted values are resistivity recalculated including the change of volume (index CO, compensation for volume expansion) for DSC and again pulse heating measurements.

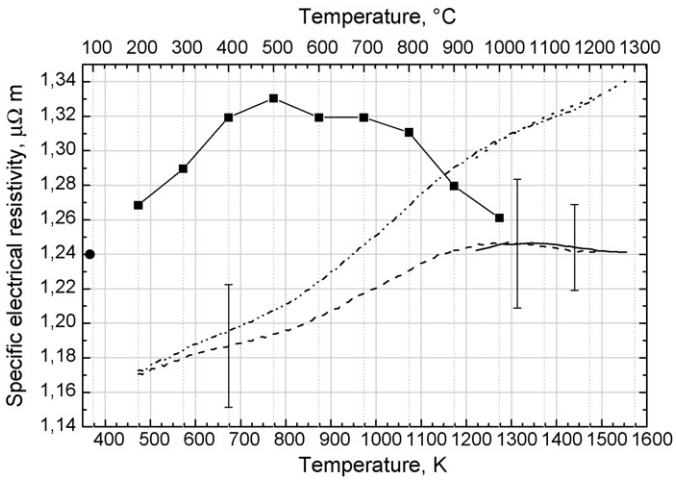

Fig. 4. Specific electrical resistivity without (ρ_{IG}, dashed line) and with (ρ_{CO}, dashed-dot-dot line) considering volume expansion in the solid state. (full line) Pulse heating data without considering volume expansion; (dotted line) pulse heating data considering volume expansion; (circle) single value at room temperature from ASM Handbook [7]; (connected squares) data from Betteridge and Heslop [6].

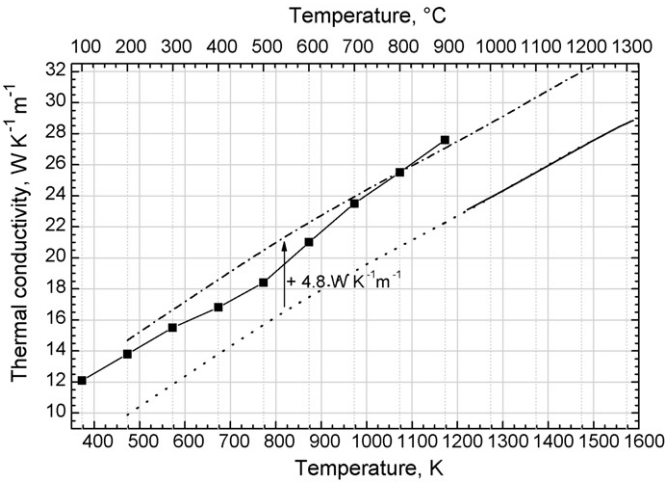

Fig. 5. Thermal conductivity in the solid state estimated via the Wiedemann–Franz law. (dotted line) Assigned temperature from DSC; (full line) assigned temperature from pulse heating; (squares) literature date from Betteridge and Heslop [6]; (dot-dashed line) constant value for lattice contribution to thermal conductivity concerning Klemens and Williams [8] added to own measurement.

For specific electrical resistivity the datapoints given in Table 3 are obtained.

Corresponding to the peaks in the c_p signal (Fig. 2) also the increase of resistivity is mainly between 800 and about 1300 K. Literature data for resistivity from Betteridge and Heslop [6] show a different slope and are higher than the own measured values, but this deviation may also occur from variation in the solution-treatment conditions from the samples of this alloy.

The datapoint at low temperature is again from ASM Handbook [7].

To estimate thermal conductivity λ from the measured electrical resistivity the Wiedemann–Franz Lorenz law (2) is used. The dotted line in Fig. 5 belongs to data, where the temperature was determined from DSC results. For the full line the pyrometer in the pulse heating setup was in the operational range. The change of density is, according to the approach for compensating the resistivity data for change of volume, extrapolated from the polynomial fit (1).

Literature values from Betteridge and Heslop [6], plotted as full squares, are higher than the present measurement. As can be seen from a theoretical consideration by Klemens and Williams [8] there are two contributions to thermal conductivity of Nimonc 80A: in the case of alloys, where electrons are strongly scattered by solute atoms, the electronic conductivity is reduced and the lattice conductivity becomes more important. For Nimonic 80A a value of 4.8 W K^{-1} m^{-1} is denoted for the lattice contribution to thermal conductivity. By calculating λ from the electrical resistivity, only the influence of electrons is considered in the actual data. This is the reason why a constant value from the lattice has to be added in order to match literature data obtained by a direct measurement of thermal conductivity.

Table 3
Measured data for Nimonic 80A

T (K)	ρ_{IG} (µΩ m)	ρ_{CO} (µΩ m)	H (kJ kg^{-1})	λ (W m^{-1} K^{-1})	a_1 (m^2 s^{-1})	a_2 (m^2 s^{-1})
500	1.173	1.176	99	10.4	2.57	2.57
600	1.182	1.188	149	12.4	3.02	2.98
700	1.188	1.198	201	14.3	3.40	3.35
800	1.196	1.211	254	16.2	3.79	3.72
900	1.208	1.230	311	17.9	–	–
1000	1.220	1.251	371	19.6	–	–
1100	1.235	1.275	434	21.1	–	–
1200	1.244	1.295	506	22.7	–	–
1300	1.247	1.310	586	24.3	–	–
1320	–	–	–	–	4.77	4.87
1350	–	–	–	–	4.87	4.98
1400	1.244	1.320	653	26.0	5.02	5.02
1450	–	–	–	–	5.11	5.17
1500	1.241	1.332	720	27.6	5.41	5.38

Data from a_1 and a_2, thermal diffusivity where the apparent specific heat capacity of the first and second run is used for calculation, are not listed where strong deviations are caused by c_p.

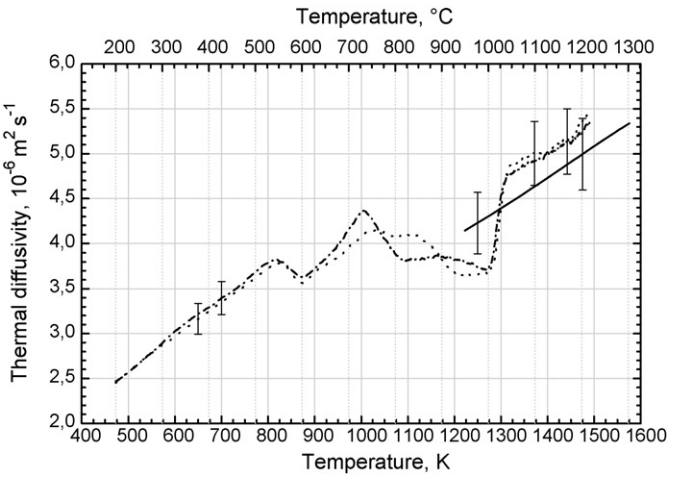

Fig. 6. Thermal diffusivity in the solid state. (dashed-dotted line) a with c_p data from first run of DSC; (dotted line) a with c_p data from second run; (bold line) a with c_p data from pulse heating.

The calculation of the thermal diffusivity a is based on the validity of the Wiedemann–Franz relationship in the stated temperature range and only the current and voltage signals from pulse heating experiments are used and the result for a is plotted in Fig. 6. Evaluation with the apparent specific heat capacity from DSC measurements results in strong deviations of a from smooth behaviour where also peaks in the c_p-curve occur from phase transitions or other processes in the material.

4. Uncertainty

According to the guide to the expression of uncertainty in measurements (GUM) [9] uncertainties reported in this paper are assigned expanded uncertainties with a coverage factor of $k = 2$. For electrical data the uncertainty budget for the pulse heating setup is given in Table 4. At the beginning of the measurement the signal of the pyrometer is very low which results in higher possible deviations at low temperatures.

For the specific heat capacity the uncertainty for temperatures below 1200 K is ± 3% and increases for higher temperatures up to ± 5%. To consider also the extrapolation of the specific heat capacity from 480 K down to room temperature to calculate the specific enthalpy, the uncertainty of $H(T)$ is ± 5% over-all given data.

Table 4
Uncertainties for the measured data from pulse heating (without considering volume expansion)

Measured data	Uncertainty, % ($k = 2$)
$H_S(T)$ in the solid phase	±5
Specific electrical resistivity with initial geometry ($\rho_{ig}(T)$)	±2
Specific heat capacity in the solid phase ($c_p(T)$)	±6
Thermal diffusivity, solid phase with DSC data ($a(T < 1200\,K)$)	±5
Thermal diffusivity, solid phase with DSC data ($a(T > 1200\,K)$)	±7
Thermal diffusivity in the solid phase with pulse heating ($a(T)$)	±8

5. Conclusion

In this study the temperature dependencies of the specific heat capacity, enthalpy, electrical resistivity, thermal conductivity, and thermal diffusivity of the Ni-based alloy Nimonic 80A has been reported and compared to literature values. The temperature dependencies could be extended down to temperatures of about 500 K. Despite the different heating rates, both methods employed in this investigation show a very good agreement of the obtained thermophysical data within the stated uncertainties of each experiment.

One has to be very careful when interpreting the thermal conductivity values of alloys, because it may occur – dependent on the experimental method used – that not all contributions to the process of thermal conductivity are taken into account. For pulse heating experiments a constant value for the lattice contribution has to be added or a calculation with an adjusted Lorentz number for the alloyed metal has to be performed. The calculated thermal diffusivity shows deviations from a smooth curve corresponding to the peaks in the c_p.

Acknowledgment

This work was supported by the Austrian "Forschungsförderungsgesellschaft mbH", Sensengasse 1, 1090 Vienna, under contract no. 810999.

References

[1] B. Wilthan, R. Tanzer, W. Schützenhöfer, G. Pottlacher, Thermophysical properties of the Ni-based alloy Nimonic 80A up to 2400 K, Rare Metals 25 (5) (2006) 529–531.
[2] B. Wilthan, K. Preis, R. Tanzer, W. Schützenhöfer, G. Pottlacher, Thermophysical properties of the Ni-based alloy Nimonic 80A up to 2400 K, II. J. Alloys Compd., in press, doi:10.1016/j.physletb.2003.10.071.
[3] K.C. Mills, B.J. Monaghan, B.J. Keene, Thermal conductivities of molten metals. Part 1. Pure Metals, NPL Report CMMT(A) (1997) p. 53.
[4] E. Kaschnitz, G. Pottlacher, H. Jäger, A new microsecond pulse-heating system to investigate thermophysical properties of solid and liquid metals, Int. J. Thermophys. 13 (4) (1992) 699–710.
[5] M. Boivineau, G. Pottlacher, Thermophysical properties of metals at very high temperatures obtained by dynamic heating techniques recent advances, Int. J. Mater. Prod. Technol. 26 (3/4) (2006) 217–246.
[6] W. Betteridge, J. Heslop, The Nimonic Alloys and Other Nickel-Base High-Temperature Alloys, Arnold, London, 1974, p. XIV.
[7] ASM Handbook, Properties and Selection: Alloy Phase Diagrams, vol. 3, ASM International (1991), in ASM Handbook on CD-ROM, ASM International and The Dialog Corporation (1999).
[8] P.G. Klemens, R.K. Williams, Thermal conductivity of metals and alloys, Int. Met. Rev. 31 (5) (1986) 197.
[9] Deutsches Institut für Normung e.V. DIN, Leitfaden zur Angabe der Unsicherheit beim Messen, 1st ed., Beuth Verlag GmbH, 1995, ISO (Geneva, Switzerland, 1993) (original: Guide to the Expression of Uncertainty in Measurement).